

UNCLASSIFIED

Defense Technical Information Center  
Compilation Part Notice

ADP012292

TITLE: Advances in the Low Temperature Preparation and Structural Characterization of Lanthanum Strontium Manganite Powder

DISTRIBUTION: Approved for public release, distribution unlimited

This paper is part of the following report:

TITLE: Applications of Ferromagnetic and Optical Materials, Storage and Magnetoelectronics: Symposia Held in San Francisco, California, U.S.A. on April 16-20, 2001

To order the complete compilation report, use: ADA402512

The component part is provided here to allow users access to individually authored sections of proceedings, annals, symposia, etc. However, the component should be considered within the context of the overall compilation report and not as a stand-alone technical report.

The following component part numbers comprise the compilation report:  
ADP012260 thru ADP012329

UNCLASSIFIED

## Advances in the Low Temperature Preparation and Structural Characterization of Lanthanum Strontium Manganite Powder

Sophie Guillemet-Fritsch, Hervé Coradin, Antoine Barnabé, Christophe Calmet, Philippe Tailhades and Abel Rousset

Centre Inter-universitaire de Recherche et d'Ingénierie des Matériaux (CIRIMAT)/  
UMR CNRS 5085, LCMIE,  
Université Paul Sabatier, Bât. 2R1-118, Route de Narbonne 31062, Toulouse Cedex, France

### ABSTRACT

Perovskite oxides of formula  $\text{La}_{1-x}\text{Sr}_x\text{MnO}_3$  have been obtained by the thermal decomposition of precursor powders. Two different kinds of precursors, carbonates and citrates have been prepared by low temperature, i.e., "chimie douce" technique. The careful control of the chemical and the hydrodynamic parameters during the synthesis process allows obtaining nice homogeneous and small size particles (80 nm for the ex-carbonates and 30 nm for ex-citrates). Pure perovskite phase is observed after a low temperature thermal treatment, from 550 °C. The structure of these oxides is either rhombohedral or cubic and depends on the strontium content, the temperature and the partial pressure of oxygen during the thermal treatment. The Mn-O distances and the Mn-O-Mn angles are directly related to the amount of  $\text{Mn}^{4+}$  content.

### INTRODUCTION

In recent years, the doped perovskite manganites such as  $\text{La}_{1-x}\text{Sr}_x\text{MnO}_3$  have attracted growing attention due to the colossal magnetoresistance (CMR) properties. Several studies have shown that the microstructure, such as grain size, plays a very significant role in the intrinsic properties [1,2]. The synthesis methods are very important to obtain polycrystalline materials with specific microstructure.

Traditional way of processing is usually the mixing of oxides, hydroxides or carbonates, followed by high temperature ( $T > 1000$  °C) processing. Consequently, the materials obtained with these methods are constituted of large particles with low surface area. "Soft chemistry" techniques have been developed in order to obtain - at lower temperature - the same materials as the one observed at high temperature with the ability to control the particle size, the surface area and the stoichiometry of the powders [3]. The advantages of using powders of reduced grain size to prepare ceramics or thick films is the increase of the reactivity and the possibility of lowering the sintering temperature. The homogeneity is a very important parameter for having reproducible properties. Our previous studies performed on spinel manganites have evidenced the influence of the powder quality on the final material properties [4, 5].

The electronic properties are related to the mixed valence state  $\text{Mn}^{3+}/\text{Mn}^{4+}$  that leads to mobile charge carriers. Low temperature synthesis allows moreover a larger oxidation state [6]. It was also observed that high oxygen ionic conductivity correlates with a cubic or an orthorhombic structure [7,8]. The coefficient of non stoichiometry  $\delta$  depends on the temperature of thermal treatment and on the oxygen partial pressure [9]. The highest values of  $\delta$  have been obtained for low temperature synthesis technique [10]. Many recent studies indicate that the  $\text{LaMnO}_{3+\delta}$  compounds exhibit different structural types as orthorhombic  $Pnma$ , rhombohedral  $R\bar{3}c$ , monoclinic  $P2_1/c$  or cubic  $Pm\bar{3}m$  phases [10-15]. These phase transitions continue to exist when the pure  $\text{LaMnO}_{3+\delta}$  is doped with divalent  $\text{Sr}^{2+}$  cations [16,17].

The aim of this work is to synthesize, by “chimie douce” technique, lanthanum strontium manganite powders of controlled characteristics (size, composition, homogeneity, surface area). These oxides are obtained from thermal decomposition of precursors (carbonates and citrates) powders. The structural evolution of  $\text{La}_{1-x}\text{Sr}_x\text{MnO}_{3+\delta}$  is studied for various compositions ( $x = 0.10, 0.30$  and  $0.50$ ), temperature and atmosphere of the thermal treatment of decomposition ( $T = 600, 900$  and  $1250^\circ\text{C}$  under air or  $\text{O}_2$  flow).

## EXPERIMENT

The powder morphology was observed with a JEOL 2010 transmission electron microscope. The thermal decomposition of the precursors was examined by thermogravimetric analyses (TGA) (SETARAM TAG 24 apparatus, accuracy  $< 10^{-6}$  g). The structure was determined by X-ray diffraction analysis : the powder X-ray diffraction (PXRD) data was collected with a SEIFERT XRD-3003-TT diffractometer using  $\text{Cu-K}\alpha$  radiation (in the range  $10^\circ \leq 2\theta \leq 140^\circ$  in increments of  $0.02^\circ$ ). The Rietveld method implemented in the program FULLPROF [18] has been used for nuclear structure refinement. Plasma emission spectrometry was used to determine the chemical composition of the oxides. The specific surface area was determined using a Micrometrics Accusorb 2100<sup>E</sup>, defined by the Brunauer, Emmet and Teller (BET) method.

Temperature programmed desorption analyses (TPD) were studied by thermogravimetry, gas chromatography and mass spectroscopy. The sample was first degassed (1 Pa) at room temperature for 1 h, and then the system was filled with Ar. A flow of  $15 \text{ cm}^3\text{min}^{-1}$  was allowed to pass through the reactor. During the experiment, the temperature was linearly increased (with a heating rate of  $5^\circ\text{Cmin}^{-1}$ ). Every 120 s, the gas flowing out of the reactor was sampled and analyzed by gas chromatography (SHIMADZU GC-8A chromatograph fitted with a molecular sieve 13X column and a thermal conductivity detector). These analyses provided the oxygen concentration in the flowing gas, and the integration of these data over time gave the total amount of oxygen released during the experiment.

## RESULTS

### Carbonate route

Carbonates are obtained by the co-precipitation of an aqueous solution of the metallic salts (lanthanum nitrate  $\text{La}(\text{NO}_3)_3 \cdot 6\text{H}_2\text{O}$ , strontium nitrate  $\text{Sr}(\text{NO}_3)_2$  and manganese nitrate  $\text{Mn}(\text{NO}_3)_2 \cdot 6\text{H}_2\text{O}$ ) with ammonium carbonate. The concentrations of the salts and of the precipitating agent are respectively  $3 \text{ mol.l}^{-1}$  and  $0.4 \text{ mole.l}^{-1}$ . The salts and the ammonium carbonate are dissolved in distilled water. The solution containing the ammonium carbonate is poured in the solution containing the metallic salts. The aging time is 30 minutes. The so obtained particles are carefully washed and dried. The thermal decomposition was then followed by TGA (**Figure 1**) and by mass spectrometry. Four phenomena can be observed. The first reaction (I) is an endothermic one and corresponds to the departure of water molecules. The next 3 steps respectively noticed at  $420^\circ\text{C}$ ,  $720^\circ\text{C}$  and  $880^\circ\text{C}$  are exothermic and were identified as the decomposition (departure of  $\text{CO}_2$  and  $\text{CO}$ ) of the simple carbonates (La and Mn). The initial powder is probably constituted of an intimate mixture of lanthanum carbonate and manganese carbonate. The strontium is substituted either in one or the other carbonate. TGA analyses show that the single phase oxide should be obtained from  $880^\circ\text{C}$ .

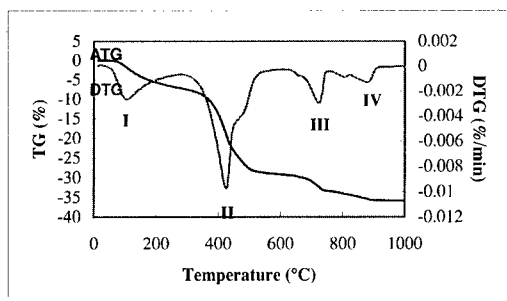


**Figure 1.** TGA and DTA curves of La-Sr-Mn carbonate decomposition

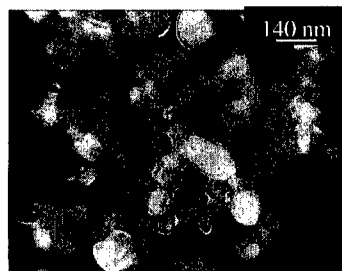


**Figure 2.** TEM micrograph of ex-carbonate  $\text{La}_{1-x}\text{Sr}_x\text{MnO}_3$  obtained at 1000 °C.

TEM observations (**Figure 2**) of an oxide of composition  $\text{La}_{0.68}\text{Sr}_{0.28}\text{Mn}_{1.04}\text{O}_4$  prepared at 1000 °C show that the oxide particles have a nice regular shape. The crystallite size determined from the broadening of the X-Ray diffraction patterns is approximately 80 nm. It does not vary as a function of the strontium content.

### Citrate route

This method of synthesis has been developed by Szabo [19]. It allows obtaining oxides with the perovskite structure at moderate temperature. The synthesis of the mixed citrate needs first to synthesis the simple citrates, La citrate, Sr citrate and Mn citrate. Lanthanum and strontium citrates are prepared by the following procedure. 0.2 moles of lanthanum (strontium) nitrate are dissolved in 600 ml of water. The solution is poured in a solution of dihydrogenocitrate dissolved in water. The solution is mixed during 1 hour and then passed through a centrifuge for 10 minutes. Thermogravimetric analyses show that the 2 citrates have the respective formula :  $\text{La}(\text{C}_6\text{H}_5\text{O}_7)$ ,  $3.5 \text{ H}_2\text{O}$  and  $\text{Sr}_3(\text{C}_6\text{H}_5\text{O}_7)_2$ ,  $3.5 \text{ H}_2\text{O}$ . A different procedure is used for the synthesis of manganese citrate. 0.5 moles of  $\text{MnO}_2$  are poured in an aqueous solution containing an excess of 0.5 moles of citric acid  $\text{C}_6\text{H}_8\text{O}_7$ ,  $6 \text{ H}_2\text{O}$ . According to Szabo [19], there is a formation of intermediate  $\text{Mn}^{4+}$  able to oxidize citric acid into acetone. The manganese ion resulting from this reaction reacts with the excess of citric acid to form the insoluble  $\text{Mn}(\text{C}_6\text{H}_5\text{O}_7)$ ,  $\text{H}_2\text{O}$  citrate. Then, the mixed La-Sr-Mn citrate is obtained after the dissolution of the simple citrates in hot ammoniacal solution. The solution is then evaporated and grounded. TGA and TPR analyses show that the heating of citrates leads to dehydration (noted I and II) and to a release of CO and  $\text{CO}_2$  (III) (**Figure 3**). The decomposition is over at 530 °C. The oxide powder is constituted of particles of approximately 30 nm (**Figure 4**).

The specific surface area was determined as a function of the thermal treatment temperature. This method of synthesis allows obtaining a specific surface area varying from 30 to  $2 \text{ m}^2/\text{g}$  as the temperature increases from 550 °C to 1000 °C. The values obtained in this work are 50 % higher than the one reported after firing precursors prepared using the Pechini process [20].

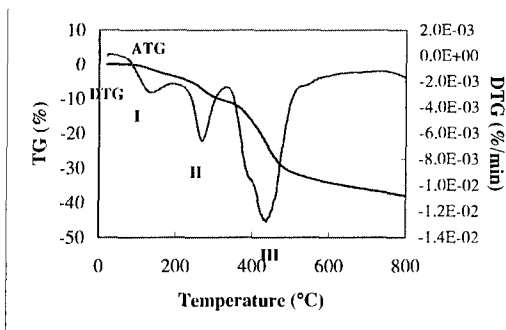


**Figure 3.** TGA and DTA curves of La-Sr-Mn citrate decomposition



**Figure 4.** TEM micrograph of an ex-citrate  $\text{La}_{1-x}\text{Sr}_x\text{MnO}_{3+\delta}$  oxide obtained at 800 °C

The structural evolution of the ex-citrates  $\text{La}_{1-x}\text{Sr}_x\text{MnO}_{3+\delta}$  oxides with  $x = 0.10, 0.30$  and  $0.50$  has been studied for various temperature and atmospheres ( $T = 600, 900$  and  $1250^\circ\text{C}$  under air or  $\text{O}_2$  flow).  $\theta$ - $2\theta$  PXRD diffractograms are registered for all the samples. The results of the structural refinements are systematically connected to the  $\text{Mn}^{4+}$  content in the samples. Additional samples of different composition and prepared at various temperature and atmosphere need to be done to complete this study and correspond to the on going research work.

For these compounds, all the structures exhibit rhombohedral or cubic symmetries with the  $R\bar{3}c$  and  $Pm\bar{3}m$  space groups respectively : no distorted perovskite phase due to a Jahn-Teller effect is observed. Lattice parameters, Mn-O distances and Mn-O-Mn angles are resumed in **Table I**. In these symmetries,  $\text{MnO}_6$  octahedra are always regular with 6 equal Mn-O distances. Therefore, Mn-O distances are an appropriate parameter to characterize the structural evolution of this series as shown in the **Figure 5** where the Mn-O distances obtained by PXRD structural refinements are plotted versus the  $\text{Mn}^{4+}$  content determined by TPD. The Mn-O-Mn angles are also presented in order to confirm the decrease of the distortion from a rhombohedral ( $a'a'a'$ ) tilted structure with  $\text{Mn-O-Mn} < 165^\circ$  to a cubic ( $a^0a^0a^0$ ) one where  $\text{Mn-O-Mn} = 180^\circ$ , according to the Glazer tilt system notation [21]. This results confirm that the lattice parameters are very sensitive to changes in the oxygen content in these pseudo-cubic perovskite compounds : for the same Sr doping ratio  $\text{La}_{0.90}\text{Sr}_{0.10}\text{MnO}_{3+\delta}$ , we can stabilize with the  $1250^\circ\text{C}/\text{air}$  decomposition conditions a really highly tilted structure with Mn-O-Mn equal to  $163^\circ$  and a nearly cubic cell with the  $700^\circ\text{C}/\text{O}_2$  conditions.

- The  $1250^\circ\text{C}/\text{air}$  compound corresponds to the limit of the tilt angle of the rhombohedral phase : no oxide presenting a rhombohedral symmetry with a more tilted Mn-O-Mn angle has been reported in the literature. Systematically, for more tilted Mn-O-Mn angle, a distortion, due to Jahn-Teller effect, appears and generates a structural transition to orthorhombic symmetry. The lattice parameter of the  $1250^\circ\text{C}/\text{air}$  compound reduced to the primary  $a_p$  cubic perovskite is very close to the  $x = 0.10$  single crystal synthesized at  $1200^\circ\text{C}$  by A. Urushibara et al. [22] which is orthorhombic. A less oxidizing atmosphere during the precursors decomposition (i.e. a lower  $\text{Mn}^{4+}$  content in the sample) can also tend to the orthorhombic phase. This rhombohedral to orthorhombic transition has been reached for an oxide obtained at  $700^\circ\text{C}$  in  $\text{N}_2$  atmosphere.

Synthesis conditions	Chemical Composition	Oxygen Content $3 + \delta$	% $\text{Mn}^{4+}$	Space Group	Lattice Parameters (Å)	Mn-O distance (Å)	Mn-O-Mn angle (°)
1250°C/air	$\text{La}_{0.86}\text{Sr}_{0.09}\text{Mn}_{1.05}$	3.04	16	$R\bar{3}c$	$a = 5.529(1)$ $c = 13.352(1)$	1.966(3)	163(1)
900°C/air	$\text{La}_{0.86}\text{Sr}_{0.09}\text{Mn}_{1.05}$	3.07	22	$R\bar{3}c$	$a = 5.5171(2)$ $c = 13.3598(6)$	1.960(3)	165(1)
600°C/air	$\text{La}_{0.86}\text{Sr}_{0.09}\text{Mn}_{1.05}$	3.10	28	$R\bar{3}c$	$a = 5.4993(4)$ $c = 13.3552(6)$	1.952(2)	167(1)
900°C/air	$\text{La}_{0.69}\text{Sr}_{0.28}\text{Mn}_{1.03}$	3.02	31	$R\bar{3}c$	$a = 5.4967(6)$ $c = 13.3602(9)$	1.947(2)	169(1)
600°C/air	$\text{La}_{0.69}\text{Sr}_{0.28}\text{Mn}_{1.03}$	3.03	33	$R\bar{3}c$	$a = 5.4932(6)$ $c = 13.351(1)$	1.946(3)	169(1)
600°C/O <sub>2</sub>	$\text{La}_{0.86}\text{Sr}_{0.09}\text{Mn}_{1.05}$	3.14	35	$R\bar{3}c$	$a = 5.487(1)$ $c = 13.323(3)$	1.940(3)	171(1)
900°C/air	$\text{La}_{0.49}\text{Sr}_{0.41}\text{Mn}_{1.09}$	3.01	42	$Pm\bar{3}m$	$a = 3.8643(2)$	1.932(1)	180
600°C/air	$\text{La}_{0.49}\text{Sr}_{0.41}\text{Mn}_{1.09}$	3.03	46	$Pm\bar{3}m$	$a = 3.8641(3)$	1.932(1)	180

**Table I.** Lattice parameters for the ex-citrates  $\text{La}_{1-x}\text{Sr}_x\text{MnO}_{3+\delta}$  oxides. The rhombohedral parameters are indicated with hexagonal axes. Estimated standard deviations are in parentheses.

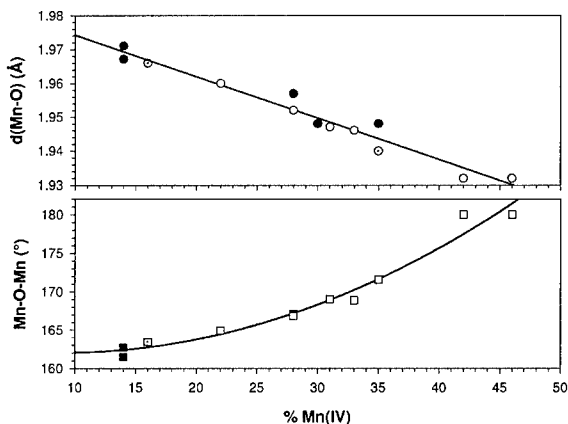


**Figure 5.** Mn-O distances and Mn-O-Mn angles as a function of  $\text{Mn}^{4+}$  content for ex-citrates  $\text{La}_{1-x}\text{Sr}_x\text{MnO}_{3+\delta}$  (with  $x \approx 0.10, 0.30$  and  $0.50$ ) and for  $T = \{1250^\circ\text{C}/\text{air}, 900^\circ\text{C}/\text{air}, 600^\circ\text{C}/\text{air}$  and  $600^\circ\text{C}/\text{O}_2\}$ . The white points correspond to this work and the black points correspond to the references [10, 15, 20].

- For the  $900^\circ\text{C}/\text{air}$ ,  $600^\circ\text{C}/\text{air}$ ,  $600^\circ\text{C}/\text{O}_2$  compounds, we can observe a decrease of the Mn-O distances coupled with an increase of the Mn-O-Mn angle leading to a less tilted phase as the  $\text{Mn}^{4+}$  increases. The symmetry is always rhombohedral even in the  $600^\circ\text{C}/\text{O}_2$  compound. The constant decrease of the distortion is strongly correlated to the  $\text{Mn}^{4+}$  content : for the same Sr doping ratio, the  $\text{Mn}^{4+}$  content can be simply reduced to the oxygen non-stoichiometry  $\delta$  in  $\text{La}_{0.90}\text{Sr}_{0.10}\text{MnO}_{3+\delta}$  formula : the  $\text{MnO}_6$  tilt system tends to decrease with the increase of  $\text{Mn}^{4+}$  and

finally attempts the perfect cubic cell for  $\text{Mn}^{4+} \geq 45\%$ . The Mn-O distances also decrease and tend to 1.93 Å. This value corresponds to the ideal cubic perovskite cell ( $a_p \approx 3.86 \text{ Å}$ ) and also to the sum of the ionic radii of  $\text{Mn}^{4+}$  ( $r_{\text{Mn}^{4+}} = 0.53 \text{ Å}$ ) and O(-II) ( $r_{\text{O}^{2-}} = 1.40 \text{ Å}$ ) [23].

- The two others oxides ( $x = 0.30$  and  $x = 0.50$ ) confirm this  $\text{Mn}^{4+}$  dependence. In these cases, the total  $\text{Mn}^{4+}$  content is mostly due to the initial Sr doping ratio rather than the non-stoichiometry in oxygen :  $\delta$  value decreases and tends to 0 when  $x$  increases. The two compounds  $\text{La}_{0.49}\text{Sr}_{0.41}\text{Mn}_{1.09}\text{O}_{3+\delta}$  are cubic.

## CONCLUSION

Lanthanum strontium manganite powders have been prepared by a "Chimie douce" process. Homogeneous particles of controlled size, size distribution and morphology have been obtained. Both the surface area and the oxygen content can be adjusted. The structure (symmetry, Mn-O distances, Mn-O-Mn angles) strongly depends on the  $\text{Mn}^{4+}$  content in the sample.

## REFERENCES

1. L.E. Huesco, F. Rivadulla, R.D. Sanchez, D. Caeiro, C. Jardon, C. Vazquez-Vazquez, J. Rivas, M.A. Lopez-Quintela, *J. Magn. Magn. Mater.* **189**, 321 (1998).
2. N. Zhang, W.P. Ding, W. Zhong, D.Y. Du, *Phys. Rev. B* **56**, 8138 (1997).
3. J. Twu, P.K. Gallagher « *Properties and applications of perovskite-type oxides* » ed. by L.G. Tejuca, J.L.G. Fierro, (1993).
4. S. Fritsch, J. Sarrias, M. Brieu, J.J. Couderc, J.L. Baudour, E. Snoeck and A. Rousset, *Solid State Ionics* **109**, 229 (1998).
5. C. Chaneel, S. Guillemet-Fritsch, J. Sarrias and A. Rousset, *Int. J. Inorg. Mat.* **2**, 24 (2000).
6. I. Maurin, P. Barboux, Y. Lassailly, J.P. Boilot, *Key Engineering Materials* **132-136**, 1357 (1997).
7. Butler V., Catlow C.R., Fender B.E.F., Harding J.H., *Solid State Ionics* **8**, 109 (1982).
8. Cook R.L., Sammells A.F., *Solid State Ionics* **45**, 311 (1991).
9. J.A.M. Van Roosmalen, E.H.P. Cordfunke and R. B. Helmholtz, *J. Solid State Chem.* **110**, 100 (1994).
10. M. Verelst, N. Rangavittal, C.N.R Rao, and A. Rousset, *J. Solid State Chem.* **104**, 74 (1993).
11. Q. Huang; A. Santoro; J.W. Lynn; R.W. Erwin; J.A. Borchers; J.L. Peng; R.L. Greene, *Phys. Rev. B* **55**, 14987 (1997).
12. J.A.M. Van Roosmalen; P. Van Vlaanderen; E.H.P. Cordfunke; W.L. IJdo, D.J.W. IJdo, *Solid State Chem.* **114**, 516 (1995).
13. J. Rodríguez-Carvajal, M. Hennion; M. Moussa; A.H. Moudden; L. Pinsard; A. Revcolevschi, *Phys. Rev. B* **57**, R3189 (1998).
14. J. Töpfer, J.B. Goodenough, *J. Solid State Chem.* **134**, 117 (1997).
15. C. Ritter, M.R. Ibarra; J.M. De Teresa; P.A. Algarabel; C. Marquina, J. Blasco, J. García; S. Oseroff, S.W. Cheong *Phys. Rev. B* **56**, 8902 (1997).
16. J.F. Mitchell, D.N. Argyriou, C.D. Potter; D.G. Hinks, J.D. Jorgensen, S.D. Bader, *Phys. Rev. B* **54**, 6172 (1996).
17. L. Pinsard, A. Revcolevschi; J. Rodríguez-Carvajal, *J. Alloy Compd* **262-263**, 152 (1997).
18. J. Rodríguez-Carvajal, *Abstracts of the Satellite Meeting on Powder Diffraction of the XV Congress of the IUCr, Toulouse, France*, 127 (1990).
19. G. Szabo, *Thesis*, Lyon (1969).
20. Y-H. Huang, Z-G. Xu, C-H. Yan, Z-M. Wang, T. Zhu, C-S. Liao, S. Gao, G-X. Xu, *Solid State Comm.* **114**, 43 (2000).
21. A.M. Glazer, *Acta Cryst. B* **28**, 3384 (1972), *Acta Cryst. A* **31**, 756 (1975).
22. A. Urushibara, Y. Moritomo, T. Arima, A. Asamitsu, G. Kido, Y. Tokura, *Phys. Rev. B* **51**, 14103 (1995).
23. R.D. Shannon, *Acta Cryst. A* **32**, 751 (1976).